Detection of Buckling in Columnar Structures by Shape Sensing with Multi-Core Optical Fibers

TAKAFUMI OGURA, MAKITO KOBAYASHI, YUE ZHAO, DANIEL LEANDRO and HIDEAKI MURAYAMA

ABSTRACT

This paper presents the results of a demonstration experiment in which helical multi-core optical fiber shape sensing was applied to detect the buckling deformation of a columnar structure, one of the most basic structures, while preventing fiber breakage. The experimental results show that the buckling deformation of a rod can be detected even when only a part of the fiber is fixed to the measurement target, suggesting its applicability to structural health monitoring of columnar structures.

INTRODUCTION

In the maintenance and operation of infrastructures, periodic nondestructive inspections have been conventionally performed. However, structural health monitoring has been proved a potential tool to improve safety and economy, by using sensors to constantly monitor the condition of structures. While visual inspection can be done for unstable and large out-of-plane deformation behaviors such as buckling, structural health monitoring based on shape monitoring methods is useful for environments where the conventional inspection is difficult to do, such as underwater or inside solid structures.

The recent development of optical fiber sensing technology that can measure strain over a wide area has made it possible to monitor deformation of structures in service, which has been difficult to measure with conventional sensors [1]. One such technologies, optical frequency domain reflectometry (OFDR), uses interference signals generated by continuously changing the wavelength of laser light from a tunable laser source into an optical fiber, to enable distributed strain measurement with a high spatial resolution [2]. OFDR-based sensor systems conventionally measure the strain along a single optical fiber, which is insufficient to provide accurate information of shape changes of the structure. Accordingly, some solutions have been developed to obtain the additional information needed to achieve shape sensing, such as the use of

Takafumi Ogura, Makito Kobayashi, Hideaki Murayama, The University of Tokyo, 7-3-1 Hongo, Bunkyo, Tokyo, Japan
Yue Zhao, LAZOC Inc., 1-5-3 Nishi-Kameari, Katsushika, Tokyo, Japan
Daniel Leandro, Public University of Navarre, Campus de Arrosadía, Pamplona, Spain

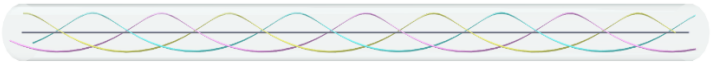

Figure 1. A schematic diagram of an MCF.

multi-core fibers (MCFs). MCFs are a type of optical fiber, initially designed for telecommunication applications, that have multiple cores arranged in the cladding. A schematic diagram of an MCF is shown in Fig. 1, showing a helical longitudinal configuration of the cores. Each core shows a linear relationship between the deformation and the strain measured, making them suitable for shape sensing and many studies have been conducted in this regard [1]. Shape sensing using multi-core optical fibers can measure the strain distribution generated in the core by capturing changes in the reflected signal from the light incident on the fiber, and can identify the three-dimensional shape of the entire fiber by geometrically calculating curve parameters from the strain of multiple cores in the fiber. Duncan et al. [3] performed 2D and 3D shape sensing by forming fiber Bragg gratings (FBGs) in a 3-core MCF and measuring the strain distribution using OFDR. An FBG is a periodic modulation of the refractive index formed in a core of an optical fiber, and by observing the shift in the Bragg wavelength of the reflected light, the strain and temperature applied to the FBG can be measured. Lally et al. [4] developed a multicore fiber with four cores arranged in a longitudinal helical configuration to solve the problem of the inability to identify the bending direction due to the twisting of the MCF, and identified right-angle bending shapes with high accuracy for a total length of 30 m by using OFDR. Westbrook et al. [5] also formed FBGs in MCFs of similar helical arrangement cores along its length and performed shape sensing also for spiral shapes.

By aligning the MCF with the object to be measured, it is expected to be possible to monitor the shape of the fiber even for nonlinear deformations such as postbuckling behavior. Tan et al. [6] attached single-mode fibers to both sides of a thin plate and used OFDR to measure and reconstruct the buckling deformation. However, if the optical fiber is bonded directly to the measurement target, it may break during large out-of-plane deformation such as buckling, limiting the application of the setup in real environments.

This paper presents an experimental demonstration to detect the buckling deformation of a columnar structure, one of the most basic structures, using a multicore optical fiber while preventing its breakage.

3D SHAPE SENSING

Maeda [7] and Kobayashi [8] formulated the relationship between the measured strain and the deformation, including torsion, of a four-core multicore fiber and designed a shape-identification algorithm. A cross section of an MCF and Frenet-Serret frame used for the shape sensing are shown in Figure 2. The process for shape-identification of a helical MCF with a central core and three

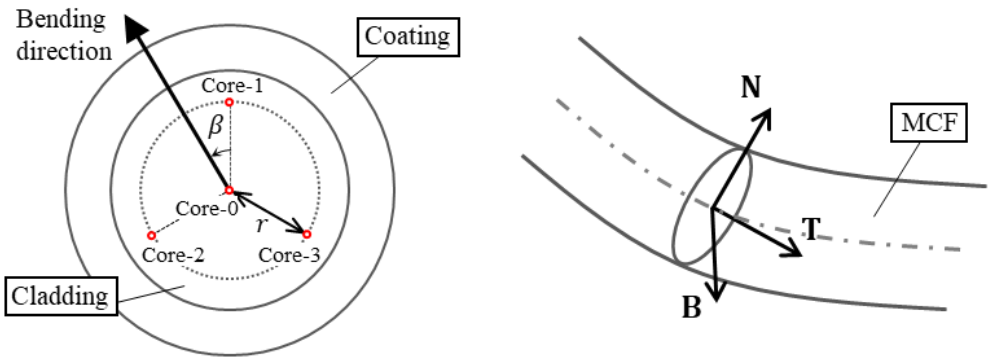

(a) A cross section of the MCF. (b) Frenet-Serret frames at the arc length *s*.

Figure 2. A cross section of an MCF and Frenet-Serret frame [7].

equally-spaced outer cores on the same circumference can be described with the following set of equations.

The true strain in the arc length s of core $i \in \{0, 1, 2, 3\}$ in a certain geometry of a helix MCF is denoted by ε_i. Core $i = 0$ is the central core and the others are the outer cores. The proportionality constants $k_{1,i}$ and $k_{2,i}$ for the angle between core i and the reference axis are defined respectively as follows:

$$k_{1,i} = \frac{1 - v(2\pi p_i r_i)^2}{(2\pi p_i r_i)^2 + 1}, \tag{1}$$

$$k_{2,i} = \frac{2\pi p_i r_i}{(2\pi p_i r_i)^2 + 1}, \tag{2}$$

where r_i is the distance of core i from the center of the MCF, p_i is the spin rate of core i, and v is the Poisson's ratio of the MCF. The specific twist angle ϕ is obtained by

$$\phi = \sum_{i=1}^{3} \frac{\varepsilon_i - k_{1,i}\varepsilon_0}{k_{2,i} r_i}. \tag{3}$$

The bending strain $\varepsilon_i^{\mathrm{bnd}}$ is given by

$$\varepsilon_i^{\mathrm{bnd}} = \varepsilon_i - k_{1,i}\varepsilon_0 - k_{2,i} r_i \phi. \tag{4}$$

The curvature κ, the bending angle β and the torsion rate τ can be derived from the following simultaneous equations with $\kappa \cos\beta$ and $\kappa \sin\beta$ as unknowns:

$$\boldsymbol{\varepsilon}^{\mathrm{bnd}} = \boldsymbol{A_1 x}, \tag{5}$$

$$\boldsymbol{\varepsilon}^{\mathrm{bnd}} = \left[\varepsilon_1^{\mathrm{bnd}} \quad \varepsilon_2^{\mathrm{bnd}} \quad \varepsilon_3^{\mathrm{bnd}}\right]^{\mathrm{T}}, \tag{6}$$

$$\boldsymbol{A_1} = \begin{bmatrix} -k_{1,1} r_1 \cos\omega_1 & -k_{1,1} r_1 \sin\omega_1 \\ -k_{1,2} r_2 \cos\omega_2 & -k_{1,2} r_2 \sin\omega_2 \\ -k_{1,3} r_3 \cos\omega_n & -k_{1,3} r_3 \sin\omega_3 \end{bmatrix}, \tag{7}$$

$$\boldsymbol{x} = [\kappa \cos\beta \quad \kappa \sin\beta]^{\mathrm{T}}. \tag{8}$$

These are solved by employing the generalized inverse:

$$\boldsymbol{x} = \left(\boldsymbol{A_1}^{\mathrm{T}}\boldsymbol{A_1}\right)^{-1}\boldsymbol{A_1}^{\mathrm{T}}\boldsymbol{\varepsilon}^{\mathrm{bnd}}. \tag{9}$$

From the above, the curvature κ and the torsion rate τ are obtained as follows:

$$\kappa = \| \boldsymbol{x} \|, \tag{10}$$

$$\beta = \mathrm{Arg}(x_1 + x_2 i), \tag{11}$$

$$\tau = \frac{d\beta}{ds}, \tag{12}$$

where β is the principal value of the argument of $\mathbf{x}$ when considered as a complex number and is 0 when $x_1 = x_2 = 0$, and the range is $(-\pi, \pi]$.

From the Frenet-Serret formula, a linear relationship is established between the Frenet-Serret frame of a curve and its derivative:

$$\frac{d\boldsymbol{v}}{ds} = \boldsymbol{A_2 v}, \tag{13}$$

$$\boldsymbol{v} = [\boldsymbol{t} \quad \boldsymbol{b} \quad \boldsymbol{n}]^{\mathrm{T}}, \tag{14}$$

$$\boldsymbol{A_2} = \begin{bmatrix} 0 & \kappa & 0 \\ -\kappa & 0 & \tau \\ 0 & -\tau & 0 \end{bmatrix}, \tag{15}$$

where $\boldsymbol{t}$ is the tangential unit vector, $\boldsymbol{n}$ is the unit vector of variation of $\boldsymbol{t}$ with respect to arc length, and $\boldsymbol{b}$ is the outer product of $\boldsymbol{t}$ and $\boldsymbol{n}$. Assuming that the curvature κ and the torsional rate τ are constant in a section with respect to the arc length, the Frenet-Serre formula is discretized as

$$\boldsymbol{v}(s + \Delta s) = \exp(\boldsymbol{A_2}\Delta s)\, \boldsymbol{v}(s). \tag{16}$$

The discretization formula of Frenet-Serret is extended to be a recurrence relation. To obtain the position vector $\boldsymbol{p}$, the tangent vector $\boldsymbol{t}$ should be integrated by the arc length, and the shape is obtained from the end for which the boundary conditions are clear to the opposite end by the recurrence relation.

MATERIALS AND METHODS

A demonstration experiment of shape sensing of buckling using a helical MCF was conducted using a column structure. The experimental configuration is shown in Figure 3, the buckling apparatus in Figure 4, and the specimen specifications in Figure 5. To prevent the MCF from breaking when buckling, a self-lubricating polytetrafluoroethylene (PTFE) tube was attached to the specimen, through which the MCF was passed and only partially fixed to the rod. A solid aluminum alloy (A6063) rod, 900 mm long and 5 mm in diameter, was

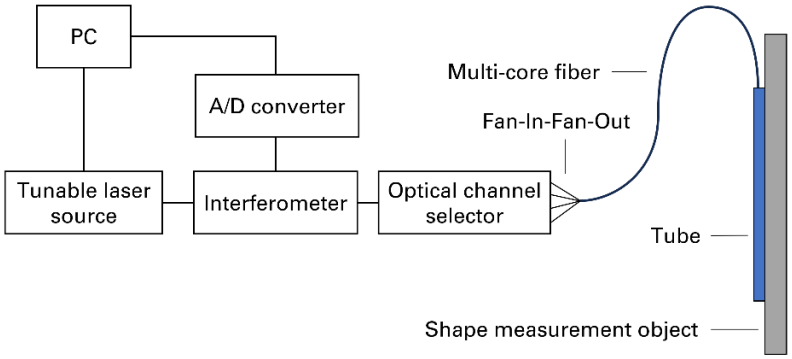

Figure 3. The experimental setup.

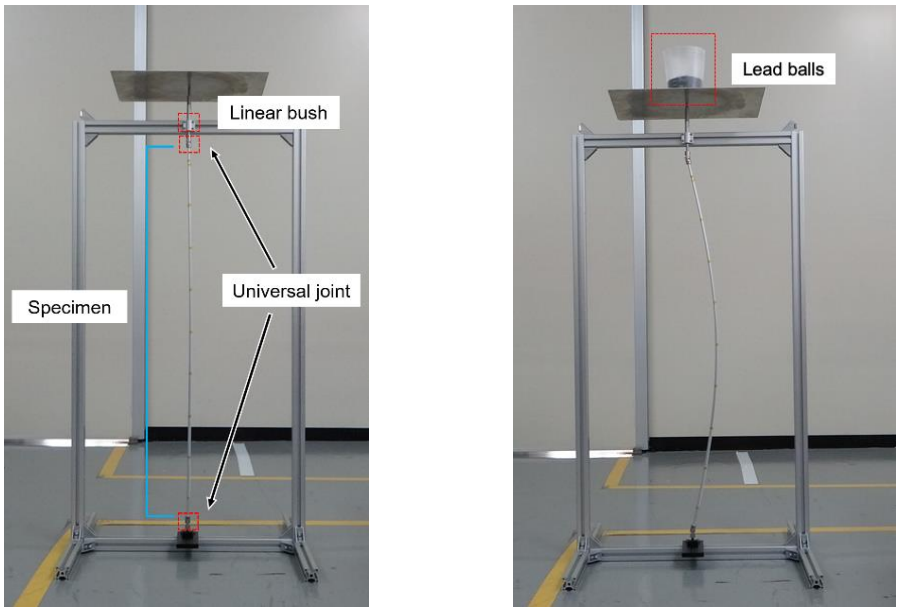

(a) The configuration of the apparatus. (b) Appearance in buckling.

Figure 4. The buckling apparatus.

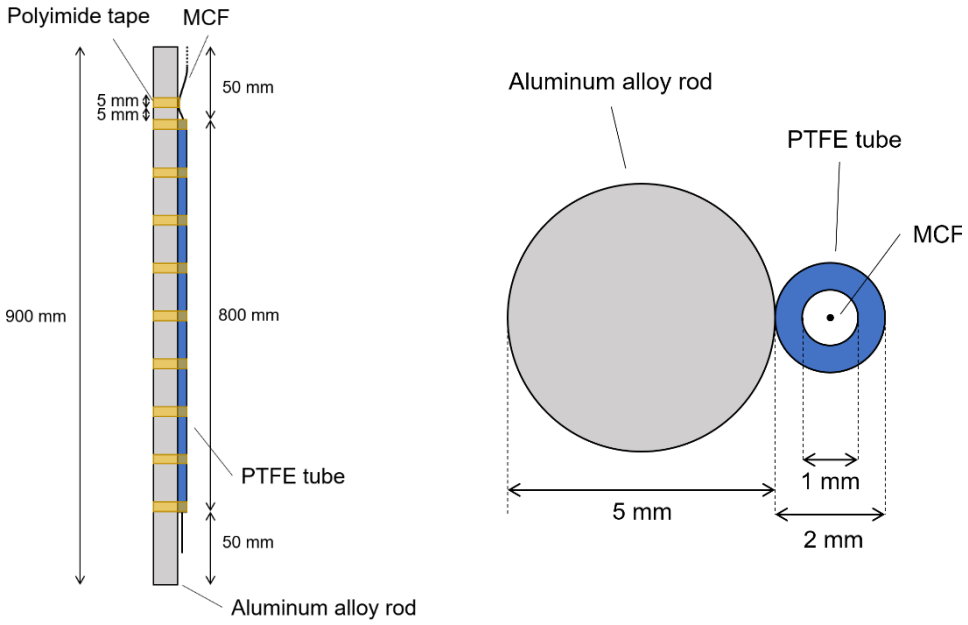

(a) Side view. (b) Overhead view.

Figure 5. The specification of the test specimen.

used as the specimen, with a PTFE tube 800 mm long, 2 mm outer diameter, and 1 mm inner diameter attached to the center along the longitudinal axis. The tube was attached to the rod with 5 mm wide polyimide tape at nine equally spaced locations, including at both ends. The MCF was passed through the tube and 5 mm of the MCF was fixed to the rod with polyimide tape from 5 mm above the top of the tube to serve as a reference for the direction of deformation during 3D shape sensing. The direction of buckling was controlled by attaching universal joints to both ends of the specimen so that the direction of rotation could be set as desired. A vertical downward load was applied to the specimen from the top of the frame via a linear shaft through a linear bush. The load was increased until buckling was achieved by gradually adding lead balls with a diameter of 2 mm to a container placed on a stand connected to the linear shaft.

Before and after buckling, the strain distributions in the center core of the fiber and in the three cores located 120 degrees apart on the outside were measured by an OFDR. The MCF used was a helical MCF with a central core and seven external cores, with a total length of 10 m, a helix pitch of 20 mm, a distance between the center and outside cores of 35 μm, and uniform grating with a center wavelength of 1550 nm. The OFDR interferometer used was a LAOFDR1500C1 manufactured by LAZOC, which can measure with a spatial resolution of 0.6 mm. Since this OFDR measurement system can measure only one channel at a time, each core was switched and measured in turn using Anritsu's MN9662A Optical Channel Selector. The tunable laser source was a TLB-6600 manufactured by Newport, and the incident light was swept at 100 nm/s from 1545 nm to 1555 nm. The specimen was buckled by setting the angle clockwise from above with the buckling direction of the specimen as 0° and changing the fixing angle of the specimen so that the surface to which the tube is attached is 0°, 90°, 180°, and 270°, respectively. The signals observed by the interferometric system were processed by STFT to obtain the wavelength shifts before and after buckling deformation at each position, which were converted to strain distributions. The curve parameters of the MCF were calculated from the strain distributions of the four cores measured, and the shape was estimated starting from the area fixed to the rod.

RESULTS

The measured strains when the specimens were buckled under each condition are shown in Fig. 5. The center core of the MCF is defined as core-0, and the three of the six outer cores located 120 degrees apart on the outside are defined as core-1, core-2, and core-3. In all conditions, strains of ±30 με were observed, but when the specimen was buckled in the 180-degree direction, periodic fluctuations in amplitude were observed. This may be due to the undulation of the tube caused by taping the tubes to the specimen at equal intervals. Fig. 6 shows the results of estimating the shape of the MCF by calculating the curve parameters from the measured strain. Note that the shape reconstruction results start in the middle of the specimen deformation because the MCF is aligned to the middle of the specimen. The results reflect each deformation according to the relative positions of the MCF, and it can be said that the buckling was detected.

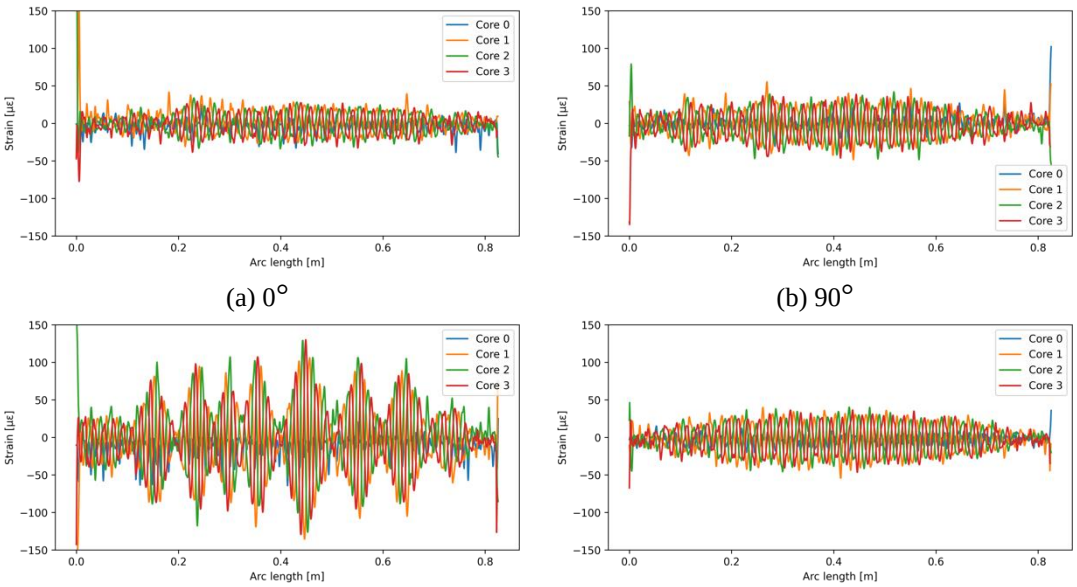

(a) 0° (b) 90°

(c) 180° (d) 270°

Figure 6. Measured strain distributions.

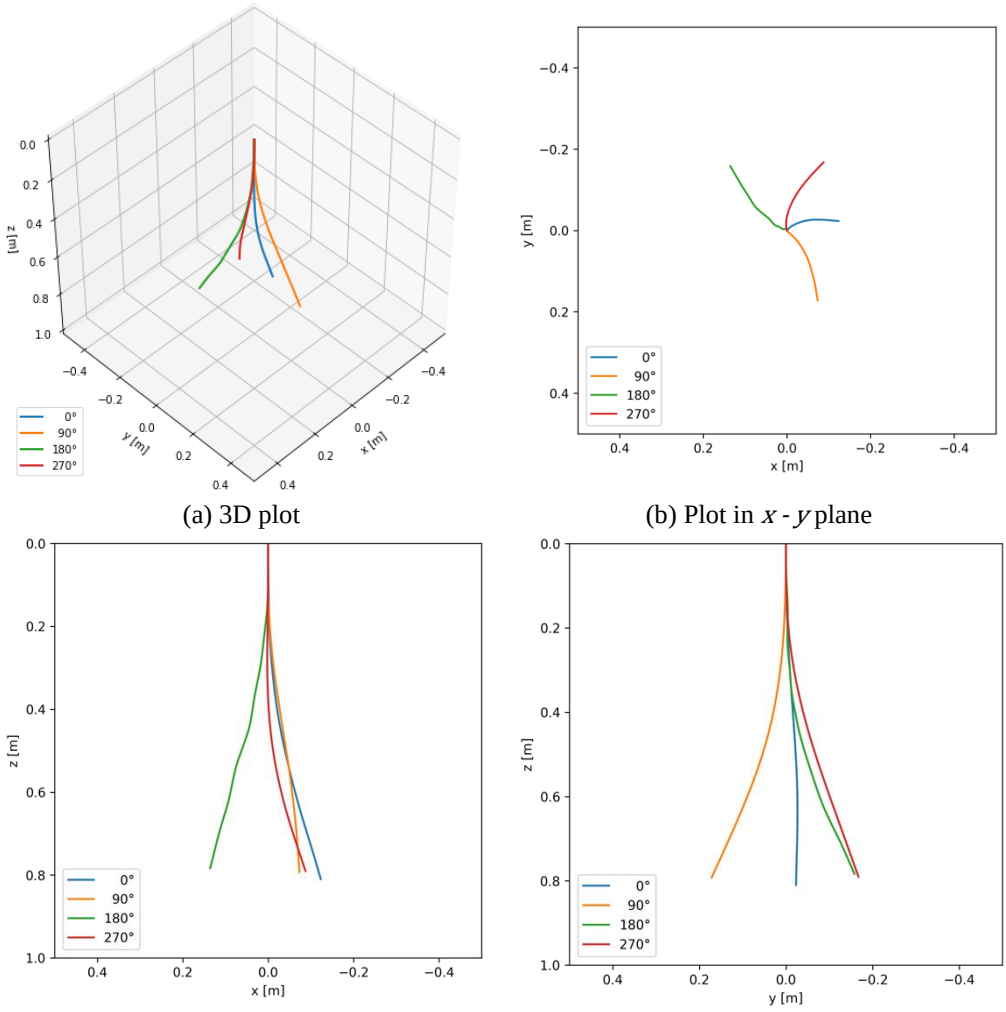

(a) 3D plot (b) Plot in x - y plane

(c) Plot in x - z plane (d) Plot in y - z plane

Figure 7. Results of shape estimation.

CONCLUSIONS

In this study, strain distributions of a helical MCF partially fixed to a columnar object were measured by OFDR to demonstrate shape sensing during buckling deformation. The experimental results suggest that the shape and direction of buckling can be detected by this method. Although the applicability of this method was demonstrated, it is expected that its accuracy will be evaluated in the future.

REFERENCES

1. Floris, I., Adam, J.M., Calderón, P. A., and Sales, S. 2021. "Fiber Optic Shape Sensors: A comprehensive review," *Optics and Lasers in Engineering*, 139.
2. Eickhoff, W. F., and Ulrich, R. J. A. P. L. 1981. "Optical frequency domain reflectometry in single-mode fiber," *Applied Physics Letters*, 39 (9), 693–695.
3. Duncan, R. G., and Raum, M. T. 2006. "Characterization of a fiber-optic shape and position sensor," *Proc. SPIE 6167, Smart Structures and Materials 2006: Smart Sensor Monitoring Systems and Applications*, 616704.
4. Lally, E. M., Reaves, M., Horrell, E., Klute, S., and Froggatt, M. E. 2012. "Fiber optic shape sensing for monitoring of flexible structures," *Proc. SPIE 8345, Sensors and Smart Structures Technologies for Civil, Mechanical, and Aerospace Systems 2012*, 83452Y.
5. Westbrook, P. S., Feder, K. S., Kremp, T., Ko, W., Wu, H., Monberg, E., Simoff, D., Bradley, K., and Ortiz, R. 2017. "Distributed sensing over meter lengths using twisted multicore optical fiber with continuous Bragg gratings," *Furukawa Electric Review*, 48, 26-32.
6. Tan, X., Guo, P., Zou, X. and Bao, Y. 2022. "Buckling detection and shape reconstruction using strain distributions measured from a distributed fiber optic sensor," *Measurement*, 200, 111625.
7. Maeda, Y., Kobayashi, M., Toh, K., Hanzawa, N., Koizumi, K., Murai, H., Wada, R., Matsui, T., Nakajima, K., and Murayama, H. 2020. "Shape Sensing for Large-scale Line Structures with Multi-core Fibers by Using Brillouin OTDR," in *Optical Fiber Sensors*, Optica Publishing Group, p. T3. 39.
8. Kobayashi, M. 2021. "Shape sensing based on strain measurements and its applications," Doctoral dissertation, The University of Tokyo.